

Recent change of vegetation growth trend in China

This article has been downloaded from IOPscience. Please scroll down to see the full text article.

2011 Environ. Res. Lett. 6 044027

(<http://iopscience.iop.org/1748-9326/6/4/044027>)

View [the table of contents for this issue](#), or go to the [journal homepage](#) for more

Download details:

IP Address: 162.105.23.151

The article was downloaded on 23/12/2011 at 01:56

Please note that [terms and conditions apply](#).

Recent change of vegetation growth trend in China

Shushi Peng¹, Anping Chen², Liang Xu³, Chunxiang Cao⁴,
Jingyun Fang¹, Ranga B Myneni³, Jorge E Pinzon⁵, Compton J Tucker⁵
and Shilong Piao¹

¹ College of Urban and Environmental Sciences, Peking University, Beijing 100871, People's Republic of China

² Department of Ecology and Evolutionary Biology, Princeton University, Princeton, NJ 08544, USA

³ Department of Geography and Environment, Boston University, 675 Commonwealth Avenue, Boston, MA 02215, USA

⁴ Institute of Remote Sensing Application of Chinese Academy of Sciences, Datun Road, 10 Beijing, People's Republic of China

⁵ NASA/Goddard Space Flight Center, Greenbelt, MD 20771, USA

E-mail: slpiao@pku.edu.cn

Received 19 October 2011

Accepted for publication 30 November 2011

Published 22 December 2011

Online at stacks.iop.org/ERL/6/044027

Abstract

Using satellite-derived normalized difference vegetation index (NDVI) data, several previous studies have indicated that vegetation growth significantly increased in most areas of China during the period 1982–99. In this letter, we extended the study period to 2010. We found that at the national scale the growing season (April–October) NDVI significantly increased by 0.0007 yr^{-1} from 1982 to 2010, but the increasing trend in NDVI over the last decade decreased in comparison to that of the 1982–99 period. The trends in NDVI show significant seasonal and spatial variances. The increasing trend in April and May (AM) NDVI (0.0013 yr^{-1}) is larger than those in June, July and August (JJA) (0.0003 yr^{-1}) and September and October (SO) (0.0008 yr^{-1}). This relatively small increasing trend of JJA NDVI during 1982–2010 compared with that during 1982–99 (0.0012 yr^{-1}) (Piao *et al* 2003 *J. Geophys. Res.—Atmos.* **108** 4401) implies a change in the JJA vegetation growth trend, which significantly turned from increasing (0.0039 yr^{-1}) to slightly decreasing (-0.0002 yr^{-1}) in 1988. Regarding the spatial pattern of changes in NDVI, the growing season NDVI increased (over 0.0020 yr^{-1}) from 1982 to 2010 in southern China, while its change was close to zero in northern China, as a result of a significant changing trend reversal that occurred in the 1990s and early 2000s. In northern China, the growing season NDVI significantly increased before the 1990s as a result of warming and enhanced precipitation, but decreased after the 1990s due to drought stress strengthened by warming and reduced precipitation. Our results also show that the responses of vegetation growth to climate change vary across different seasons and ecosystems.

Keywords: climate change, NDVI, vegetation growth, drought, grassland, desert, vegetation greening, vegetation browning, turning point, China

 Online supplementary data available from stacks.iop.org/ERL/6/044027/mmedia

1. Introduction

Vegetation growth is strongly influenced by climate change (e.g. Myneni *et al* 1997, Zhou *et al* 2001, Goetz *et al* 2005, Piao *et al* 2010). Using satellite-derived normalized difference vegetation index (NDVI) datasets, previous studies have found that vegetation growth significantly increased in most areas of China during the period 1982–99 and that the increased vegetation growth was significantly correlated with increased temperature (e.g. Zhou *et al* 2001, Piao *et al* 2003). The increased temperature boosted vegetation growth through an increase in growing season length and enhanced photosynthesis (e.g. Zhou *et al* 2001, Slayback *et al* 2003, Piao *et al* 2006a).

However, recent studies have raised a question on whether the increasing trend in China's vegetation activity will persist in the 21st century given possible changes in the climate drivers (e.g. Hansen *et al* 2010, Piao *et al* 2010). Several recent studies have suggested a decline in vegetation growth due to the widespread drought since the mid or late 1990s across the northern hemisphere, including some parts of China (e.g. Angert *et al* 2005, Goetz *et al* 2005, Park and Sohn 2010, Zhang *et al* 2010, Zhao and Running 2010, Jeong *et al* 2011, Piao *et al* 2011), but the linkage between climate change and vegetation growth in China has not been adequately quantified because these studies focused mainly on vegetation responses to climate change at a continental scale. For example, most of the previous studies (except Goetz *et al* 2005) did not investigate whether the changes in vegetation growth differed among different vegetation types. Furthermore, most of these studies were based on coarse resolution climate data, and fine scale regional ground observations have not been adequately incorporated in such studies. This suggests that a more thorough regional investigation is needed to better understand how China's vegetation activities have responded to recent changes in climates. Therefore, the first goal of this letter is to determine whether the general increase in vegetation activity over China has persisted in the new century, or whether there is a turning point beyond which the trend in vegetation activity has stalled or even reversed.

Besides the pronounced general trends in climate change, remarkable variations in seasonal trends and spatial patterns were also detected in China (Piao *et al* 2010). For example, during the past five decades, the most prominent warming trend is found in northern China (including northeastern China and Inner Mongolia) where water is limited, which, along with the concurrent decrease in precipitation, may enhance evapotranspiration and strengthen the drought stress already imposed in this region. By contrast, southern China has experienced a moderate increase in both temperature and precipitation. Seasonal variations in climate trend are also pronounced. For instance, from 1961 to 2006, spring temperature increased at a rate of 0.2 °C per decade, which is twice the rate of summer temperature increase (0.1 °C per decade) (Ding *et al* 2007, Piao *et al* 2010). The distinct temporal and spatial variations in climate may result in a strong temporal and spatial

pattern of vegetation activity considering the well-recognized association between vegetation growth and climate (Zhou *et al* 2001, 2003, Angert *et al* 2005, Piao *et al* 2011). Previous studies suggested that vegetation growth in China increased faster in spring (0.0018 yr⁻¹) than in summer (0.0012 yr⁻¹) and autumn (0.0009 yr⁻¹) from 1982 to 1999 (Piao *et al* 2003), but no efforts have been made to investigate the sensitivity of vegetation growth to climate change for different seasons. Hence, our next goal is to understand how the trends in vegetation growth vary across different seasons and regions and what the controls are behind these observed variations.

2. Datasets and methods

2.1. Datasets

Normalized difference vegetation index (NDVI) is a vegetation index to measure vegetation greenness and is proven to be positively correlated with productivity (Myneni *et al* 1997, Bunn and Goetz 2006). In this study, we used the NOAA/AVHRR NDVI composites at a spatial resolution of 0.083° and 15 day interval produced by the Global Inventory Modeling and Mapping Studies (GIMMS) (Tucker *et al* 2005) for the period 1982–2010 to explore vegetation activity. The GIMMS NDVI datasets have been corrected to minimize the effects of volcanic eruptions, solar angle and sensor errors and shifts and thus can be used to evaluate the long-term trends in vegetation activity (Zhou *et al* 2001, Slayback *et al* 2003). They were also proved to be one of the best products to depict the temporal change of vegetation growth (Beck *et al* 2011). To reduce the noise (e.g. cloud cover) in the NDVI data, we derived monthly NDVI from two images for each month using the maximum value composite (MVC) method (Holben 1986). Pixels with average annual NDVI less than 0.05 were considered as non-vegetated areas and thus removed in this study.

Our analysis was confined to the growing season, which was defined as from April to October to be consistent within the whole country (Zhou *et al* 2001, Piao *et al* 2011). It should be noted that the actual growing season may be different from that defined in this study. For instance, it is usually longer than our definition for subtropical southern China. The spatial pattern of average NDVI from April to October is shown in figure S1 (available at stacks.iop.org/ERL/6/044027/mmedia). To further understand the seasonal contributions, we divided the growing season into three seasons: April and May (AM), June, July and August (JJA) and September and October (SO), and calculated average monthly composite NDVI for each season (Zhou *et al* 2001).

Monthly surface air temperature and precipitation at a spatial resolution of 0.1° were generated using a kriging interpolation algorithm from daily temperature and precipitation records from 728 meteorological stations across China (National Meteorological Information Center of China Meteorological Administration, www.nmic.gov.cn, Piao *et al* 2003, Ding *et al* 2007). Using a nearest neighbor resampling method, we resampled the monthly surface air temperature and precipitation to a spatial resolution of 0.083° to be

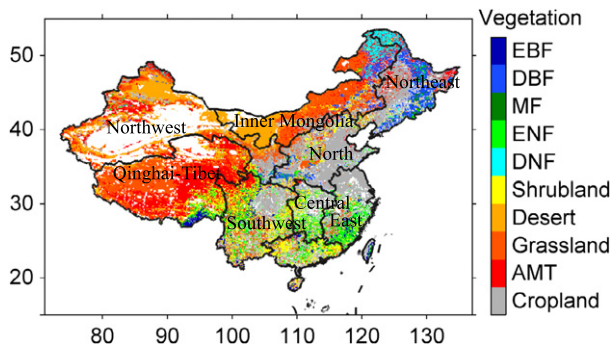


Figure 1. Vegetation map of China. EBF, DBF, MF, ENF, DNF and AMT stand for evergreen broadleaf forests, deciduous broadleaf forests, broadleaf and needleleaf mixed forests, evergreen needleleaf forests, deciduous needleleaf forests and alpine meadows and tundra, respectively.

consistent with the NDVI dataset. The spatial patterns of average growing season temperature and precipitation from 1982 to 2010 are shown in figure S1 (available at stacks.iop.org/ERL/6/044027/mmedia).

The spatial distribution of vegetation was obtained from a digitized vegetation map of China at a scale of 1:1000 000 (Editorial Editorial Board of Vegetation Map of China 2001). Ten vegetation types were recognized, i.e., evergreen broadleaf forests (EBF), deciduous broadleaf forests (DBF), broadleaf and needleleaf mixed forests (MF), evergreen needleleaf forests (ENF), deciduous needleleaf forests (DNF), shrubland, desert, grassland, alpine meadows and tundra (AMT), and cropland. Figure 1 shows the spatial distribution of the 10 vegetation types in China with a spatial resolution of 0.083°. In addition, we divided the whole country into nine regions for convenience of description (figure 1).

2.2. Analyses

To detect whether the increasing trend of China’s vegetation activity has significantly changed, we fitted and compared two regression models. The first one (equation (1)) assumes only one trend (β_1) over the entire study period, and the second one (equation (2)) is a piecewise regression model (Toms and Lesperance 2003) that assumes a significant change in the trend of NDVI time-series data (e.g. Wang *et al* 2011, Piao *et al* 2011).

$$y = \beta_0 + \beta_1 t + \varepsilon \tag{1}$$

$$y = \begin{cases} \beta_0 + \beta_1 t + \varepsilon & (t \leq \alpha) \\ \beta_0 + \beta_1 t + \beta_2(t - \alpha) + \varepsilon & (t > \alpha) \end{cases} \tag{2}$$

where y is the growing season NDVI or NDVI for each season, t is the year, α is the turning point (TP) of the NDVI time-series, β_0 , β_1 , and β_2 are regression coefficients (β_0 : intercept; β_1 : magnitude of NDVI trend before the TP; $\beta_1 + \beta_2$: magnitude of NDVI trend after the TP), and ε is the residual random error. We fitted the models to the NDVI time-series data using the maximum likelihood (least-squares error) method and evaluated them with the Akaike information criterion (AIC)

$$AIC = n \log(RSS/n) + 2k + 2k(k + 1)/(n - k - 1) \tag{3}$$

where RSS is the residual sum of squares for the estimated model, k is the number of parameters, and n is the sample size. We defined $\delta AIC = AIC_2 - AIC_1$, where AIC_1 and AIC_2 are the AIC values of model 1 and model 2, respectively. It is a rule of thumb that one model is significantly preferred over the alternatives if its AIC value is reduced by more than 2 (Burnham and Anderson 2002). Therefore $\delta AIC < -2$ favors model 2 (piecewise regression model), and $\delta AIC > 2$ favors model 1 (linear regression model).

In addition, we also calculated the trends in temperature and precipitation over the entire period, and the trends before and after the turning point of the NDVI if a significant NDVI trend change had been proven with the AIC method. To investigate the potential climatic drivers of NDVI trends, we further calculated Pearson correlation coefficients between the NDVI and climatic factors (temperature and precipitation). The same analyses were performed at both the national scale and the biome scale.

3. Results and discussion

3.1. Change in NDVI at the national scale and its association with climate change

3.1.1. Growing season NDVI. At the national scale, for the average growing season NDVI, the linear regression model (model 1) predicts a significant increasing trend of 0.0007 yr⁻¹ from 1982 to 2010 ($R^2 = 0.40$, $P < 0.001$), while fitting the piecewise regression model shows a trend change from a significant increase of 0.0029 yr⁻¹ ($R^2 = 0.69$, $P = 0.006$) before 1990 to a stalled trend of 0.0004 yr⁻¹ ($R^2 = 0.07$, $P = 0.238$) after 1990 (figure 2(a)). However, the information criterion of the piecewise regression model is larger than that of the linear regression model ($\delta AIC = AIC_2 - AIC_1 = 1.3$, table 1), indicating that the improving likelihood in the piecewise regression model with more parameters could not compensate for the increased complexity in comparison to the simple linear regression model. Hence, unlike most regions of Eurasia and North America where the increasing trend of growing season NDVI has been reversed or stalled since the late 1990s (Wang *et al* 2011, Piao *et al* 2011), there is no compelling evidence to reject the hypothesis that China’s growing season vegetation activity has kept increasing.

National average growing season NDVI is positively correlated with temperature ($r = 0.56$, $P = 0.002$) but not with precipitation ($r = 0.12$, $P = 0.526$) (figure 2(a)). Temperature increased by 0.045 °C yr⁻¹ from 1982 to 2010 ($R^2 = 0.69$, $P < 0.001$). Meanwhile, growing season precipitation did not change much from 1982 to 2010 (-0.19 mm yr⁻¹, $R^2 = 0.00$, $P = 0.766$). Therefore, the overall increase in growing season NDVI over the entire study period may be due to the increase in temperature.

3.1.2. NDVI changes in different seasons. When looking into the patterns of the AM, JJA and SO seasons (table 1,

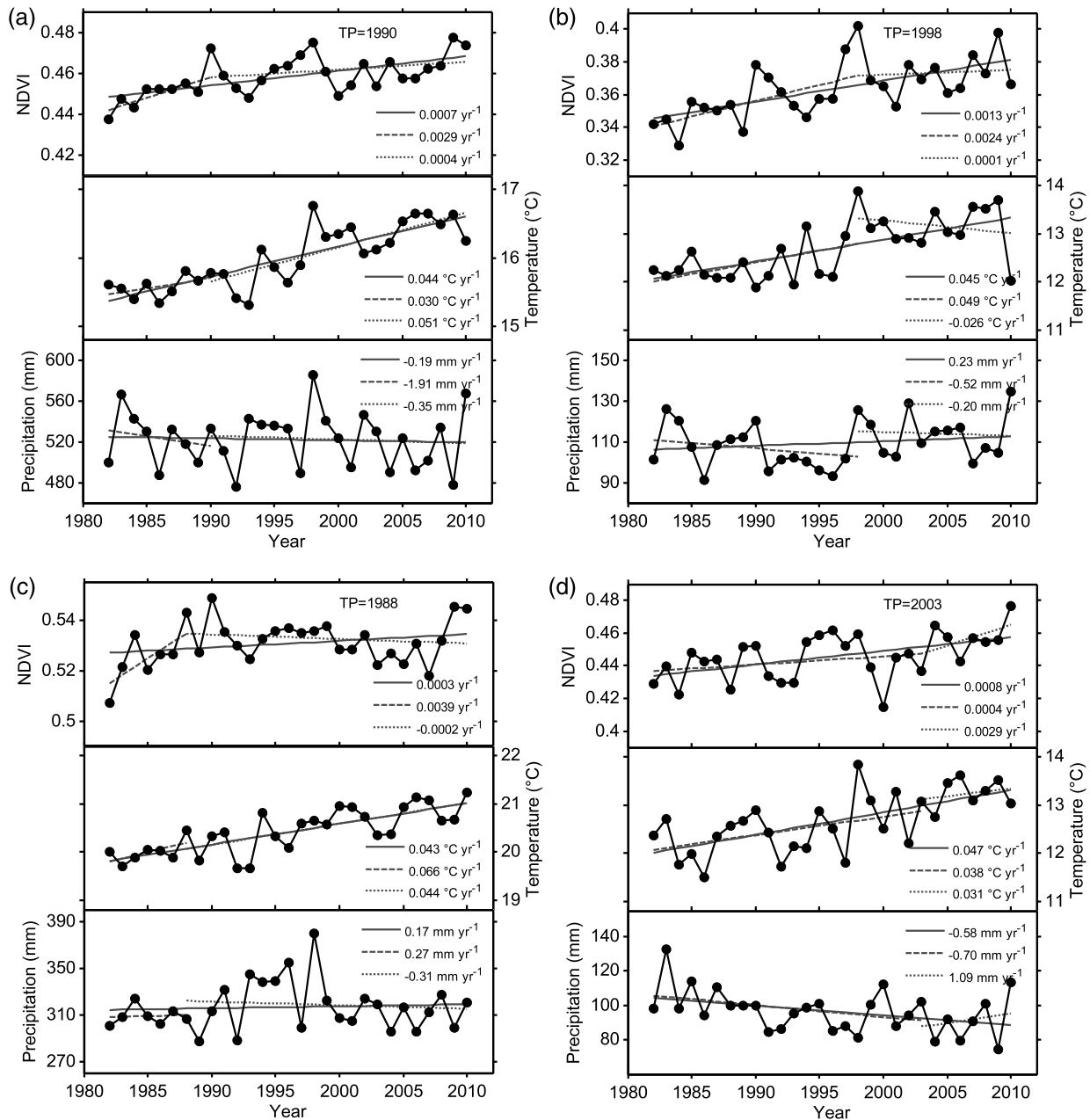


Figure 2. Inter-annual variations of (a) growing season (April–October), (b) April and May (AM), (c) June, July and August (JJA) and (d) September and October (SO) NDVI, temperature and precipitation over China. The solid lines indicate linear fits during the period 1982–2010; the dashed lines indicate linear fits before the turning point of the NDVI trend and the dotted lines indicate linear fits after the turning point of the NDVI trend. The turning point (TP) of the NDVI trend and trends estimated by least-squares linear regression are shown in the legend.

figures 2(b)–(d)), we only found a significant change in the JJA NDVI trend for which the piecewise regression model (model 2) described the NDVI trend better than the linear regression model (model 1) ($\delta AIC = -2.9$). Fitting the piecewise regression model for the JJA NDVI, we found a significant turning point of the JJA NDVI in 1988 ($P = 0.008$). Before 1988, the JJA NDVI significantly increased by 0.0039 yr^{-1} ($R^2 = 0.56, P = 0.050$), while it slightly decreased by -0.0002 yr^{-1} ($R^2 = 0.03, P = 0.416$) after 1988 (figure 2(c)). Changes in the AM and SO NDVIs are better described with the linear regression model ($\delta AIC =$

3.1 and 3.6, respectively), and they increased at rates of 0.0013 yr^{-1} and 0.0008 yr^{-1} , respectively, over the period of 1982–2010 (figures 2(b), (d); $R^2 = 0.41, P < 0.001$ for AM NDVI; $R^2 = 0.25, P = 0.006$ for SO NDVI).

The NDVIs for AM and SO are significantly and positively correlated with temperature ($r = 0.62, P < 0.001$ for AM and $r = 0.41, P = 0.027$ for SO) but not with precipitation ($r = 0.13, P = 0.504$ for AM and $r = -0.19, P = 0.316$ for SO), implying that vegetation growth is sensitive to temperature at the beginning and the end of the growing season (Richardson *et al* 2010). In addition, the rate of

Table 1. Trends in NDVI (0.01 yr^{-1}), temperature (Temp , $^{\circ}\text{C yr}^{-1}$), and precipitation (Preci , mm yr^{-1}), and precipitation (TP) of NDVI trend, difference in AIC between the piecewise regression model and the linear regression model ($\delta\text{AIC} = \text{AIC2} - \text{AIC1}$) for NDVI, trends in NDVI (0.01 yr^{-1}), temperature (Temp , $^{\circ}\text{C yr}^{-1}$), and precipitation (Preci , mm yr^{-1}) before and after the TP of the NDVI, and correlation coefficients between NDVI and temperature (R_T) and precipitation (R_P) for the growing season (April–October), April and May (AM), June, July and August (JJA) and September and October (SO) at the national scale over the period 1982–2010. * and ** stand for $P < 0.05$ and $P < 0.01$ (statistical significance of linear regression, piecewise regression or Pearson correlation), respectively.

Seasons	Trend from 1982 to 2010					Trend before TP					Trend after TP				
	NDVI (10^{-2} yr^{-1})	Temp ($^{\circ}\text{C yr}^{-1}$)	Preci (mm yr^{-1})	TP	δ AIC	NDVI (10^{-2} yr^{-1})	Temp ($^{\circ}\text{C yr}^{-1}$)	Preci (mm yr^{-1})	NDVI (10^{-2} yr^{-1})	Temp ($^{\circ}\text{C yr}^{-1}$)	Preci (mm yr^{-1})	R_T	R_P		
Growing season	0.07**	0.04**	-0.2	1990	1.3	0.29**	0.03	-1.9	0.04	0.05**	-0.4	0.56**	0.12		
AM	0.13**	0.05**	0.2	1998	3.1	0.24**	0.05	-0.5	0.01	-0.03	-0.2	0.62**	0.13		
JJA	0.03	0.04**	0.2	1988**	-2.9	0.39	0.07	0.3	-0.02	0.04**	-0.3	0.27	0.23		
SO	0.08**	0.05**	-0.6*	2003	3.6	0.04	0.04*	-0.7	0.28	0.03	1.1	0.41*	-0.19		

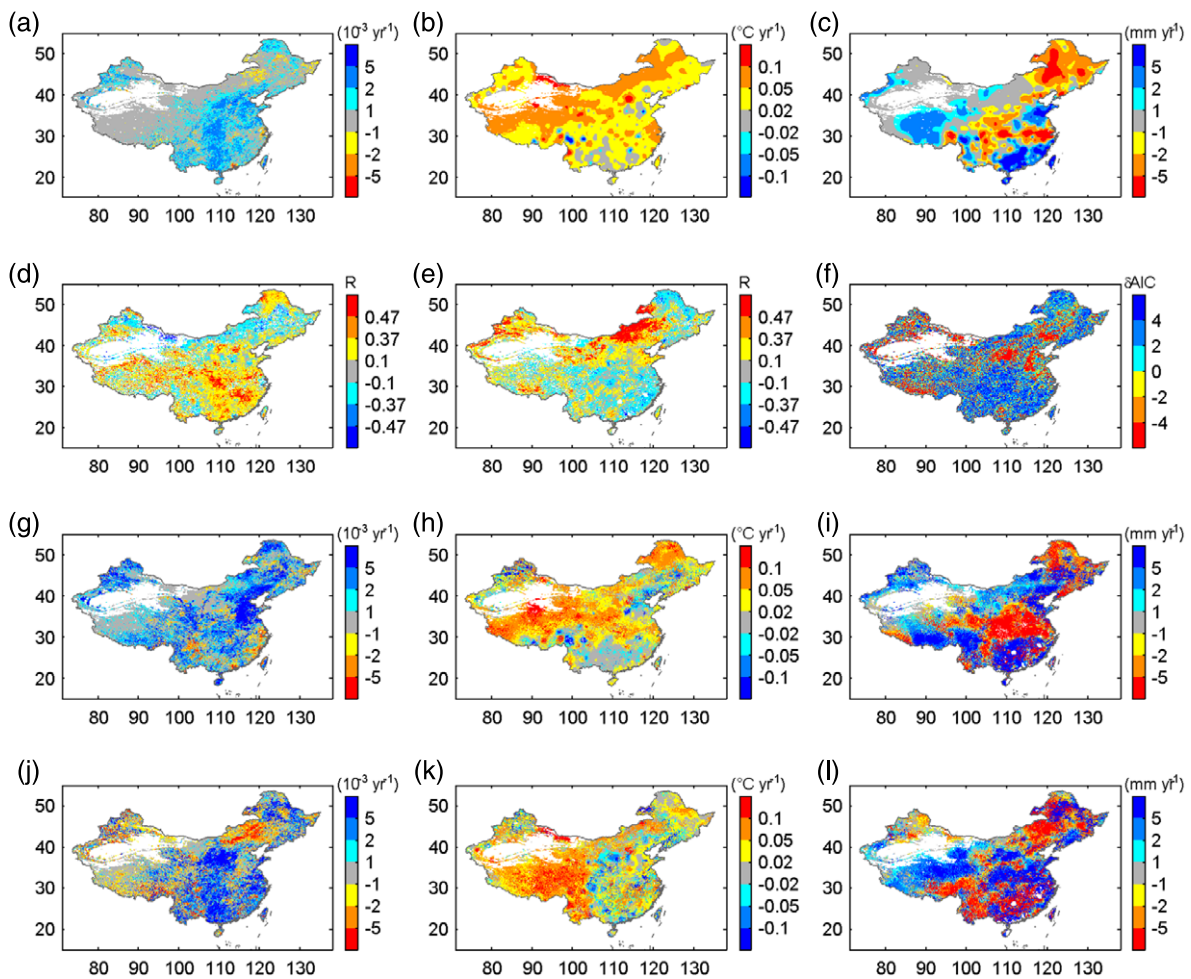


Figure 3. Spatial distribution of the results by the linear regression model and the piecewise regression model on growing season (April–October) NDVI and climate. Linear regression trends in growing season (a) NDVI, (b) temperature and (c) precipitation from 1982 to 2010. The correlation coefficients between growing season NDVI and (d) temperature and (e) precipitation. (f) Difference in AIC between piecewise regression and linear regression (ΔAIC). Trends in growing season NDVI (g) before and (j) after its TP. Trends in growing season temperature (h) before and (k) after the TP of the growing season NDVI trend. Trends in growing season precipitation (i) before and (l) after the TP of the growing season NDVI trend. $R = 0.37$ and $R = 0.47$ correspond statistically to 5% and 1% significance levels, respectively.

increase of the AM NDVI is almost twice that of the SO NDVI (figures 2(b) and (d)), despite similar magnitude of temperature change ($0.045\text{ }^{\circ}\text{C yr}^{-1}$, $R^2 = 0.41$, $P < 0.001$ for AM, and $0.047\text{ }^{\circ}\text{C yr}^{-1}$, $R^2 = 0.42$, $P < 0.001$ for SO). Hence, the sensitivity of the AM NDVI to temperature ($0.018\text{ }^{\circ}\text{C}^{-1}$) is twice that of the SO NDVI ($0.009\text{ }^{\circ}\text{C}^{-1}$). This significant difference in temperature sensitivity could be caused by the more favorable factors for vegetation growth, such as solar radiation, leaf nutrient contents, and soil water, among many others, in spring than in autumn (Sun *et al* 2003, Niu *et al* 2011). For example, Sun *et al* (2003) showed that vegetation growth is limited by light in autumn while solar radiation is generally not a limiting factor during the onset of vegetation growth in spring (Tanja *et al* 2003, Richardson *et al* 2010).

The NDVI for JJA is not statistically correlated with either temperature or precipitation ($R = 0.27$, $P = 0.158$ for temperature and $R = 0.23$, $P = 0.230$ for precipitation). In JJA, vegetation reaches peak greenness and fluctuation in temperature and precipitation has little impact on it, with the exception of severe drought suppression which is very rare

in east China. Since the trend of JJA NDVI changed from increasing to decreasing in 1988, we also calculated the JJA temperature and precipitation trend before and after 1988. The temperature of JJA increased marginally ($0.066\text{ }^{\circ}\text{C yr}^{-1}$, $R^2 = 0.38$, $P = 0.138$) from 1982 to 1988, and continued to increase significantly after 1988 ($0.044\text{ }^{\circ}\text{C yr}^{-1}$, $R^2 = 0.45$, $P < 0.001$). For the precipitation of JJA, the trends before 1988 (0.27 mm yr^{-1} , $R^2 = 0.00$, $P = 0.903$) and after 1988 (-0.31 mm yr^{-1} , $R^2 = 0.01$, $P = 0.677$) are both insignificant.

3.2. Spatial patterns of changes in NDVI and climate drivers

3.2.1. Growing season NDVI. The patterns of growing season NDVI changes are found to be spatially heterogeneous (figure 3). Comparison of statistical models indicates that the piecewise regression model works better in part of Inner Mongolia and Northeast China (figure 3(f)). In most of these regions, growing season NDVI first increased from 1982 to the 1990s, then stalled or decreased after the 1990s (figure

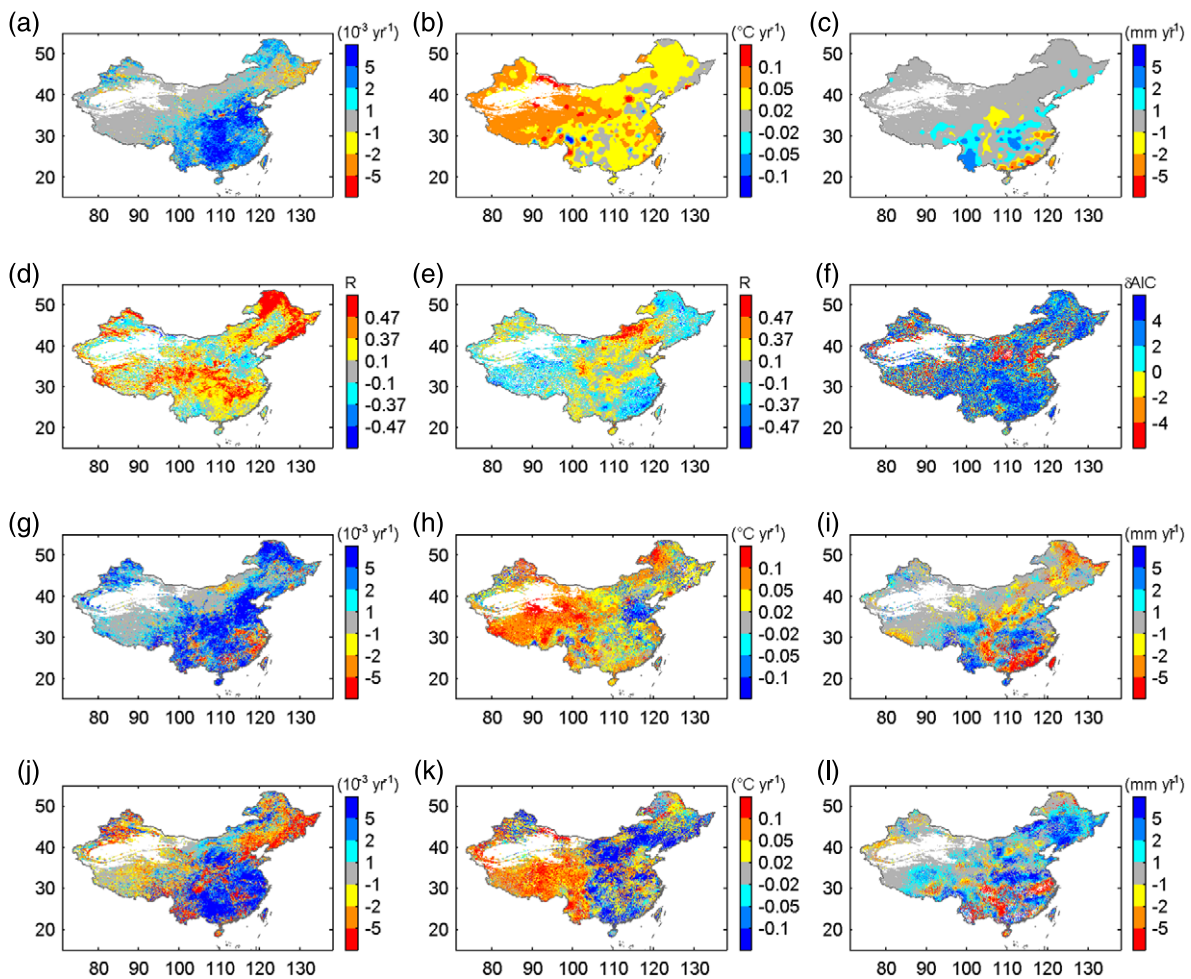


Figure 4. Spatial distribution of the results by the linear regression model and the piecewise regression model on April and May (AM) NDVI and climate. Linear regression trends in AM (a) NDVI, (b) temperature and (c) precipitation from 1982 to 2010. The correlation coefficients between AM NDVI and (d) temperature and (e) precipitation. (f) Difference in AIC between piecewise regression and linear regression (ΔAIC). Trends in AM NDVI (g) before and (j) after its TP. Trends in AM temperature (h) before and (k) after the TP of the AM NDVI trend. Trends in AM precipitation (i) before and (l) after the TP of the AM NDVI trend. $R = 0.37$ and $R = 0.47$ correspond statistically to 5% and 1% significance levels, respectively.

S2 available at stacks.iop.org/ERL/6/044027/mmedia). As a result, for these regions, the overall growing season NDVI trend is insignificant and falls in the range -0.001 to 0.001 yr^{-1} during 1982–2010 (figure 3(a)). For some other regions such as central and south China, the linear regression model with a single trend in growing season NDVI changes is more appropriate, and the growing season NDVI change is usually higher than 0.002 yr^{-1} (figure 3(a)). Overall, from 1982 to 2010, growing season NDVI increased over 73% of China’s land, and the trend is significant ($P < 0.05$) in 33% of the study area.

Figures 3(d) and (e) show the spatial patterns of correlation coefficients between growing season NDVI and growing season temperature and precipitation from 1982 to 2010. Growing season NDVI is significantly correlated with growing season temperature in the central, east and some parts of northeast China (figure 3(d)), while in the arid and semi-arid regions such as east of Inner Mongolia, the inter-annual variation of growing season NDVI is more correlated with precipitation (figure 3(e)). The continuous

increase in NDVI over southern China is consistent with the results from forest inventory (Pan *et al* 2011). Plot level forest inventory analysis (McMahon *et al* 2010) and a meta-data analysis of warming experiments from global forest and grassland sites (Lin *et al* 2010) suggested that warming could enhance forest vegetation growth. Hence, in southern China where precipitation is not a limitation for vegetation growth the increase in temperature could benefit vegetation growth.

3.2.2. Seasonal NDVI. Seasonal NDVI changes also show strong spatial heterogeneity, particularly the contrasts between northern and southern China (figures 4–6). Most of central and southern China showed a continuous increase in vegetation activity, especially in AM (figures 4(a), 5(a) and 6(a)). Yet in northern China the linear regression trend of seasonal NDVI changes across 1982–2010 is insignificant for all the three seasons, as a result of the NDVI trend reversal in the 1990s which can be better described with the piecewise regression model (figures 4(f), 5(f) and 6(f)). In addition, the NDVI trend changes for different seasons could be different in spatial

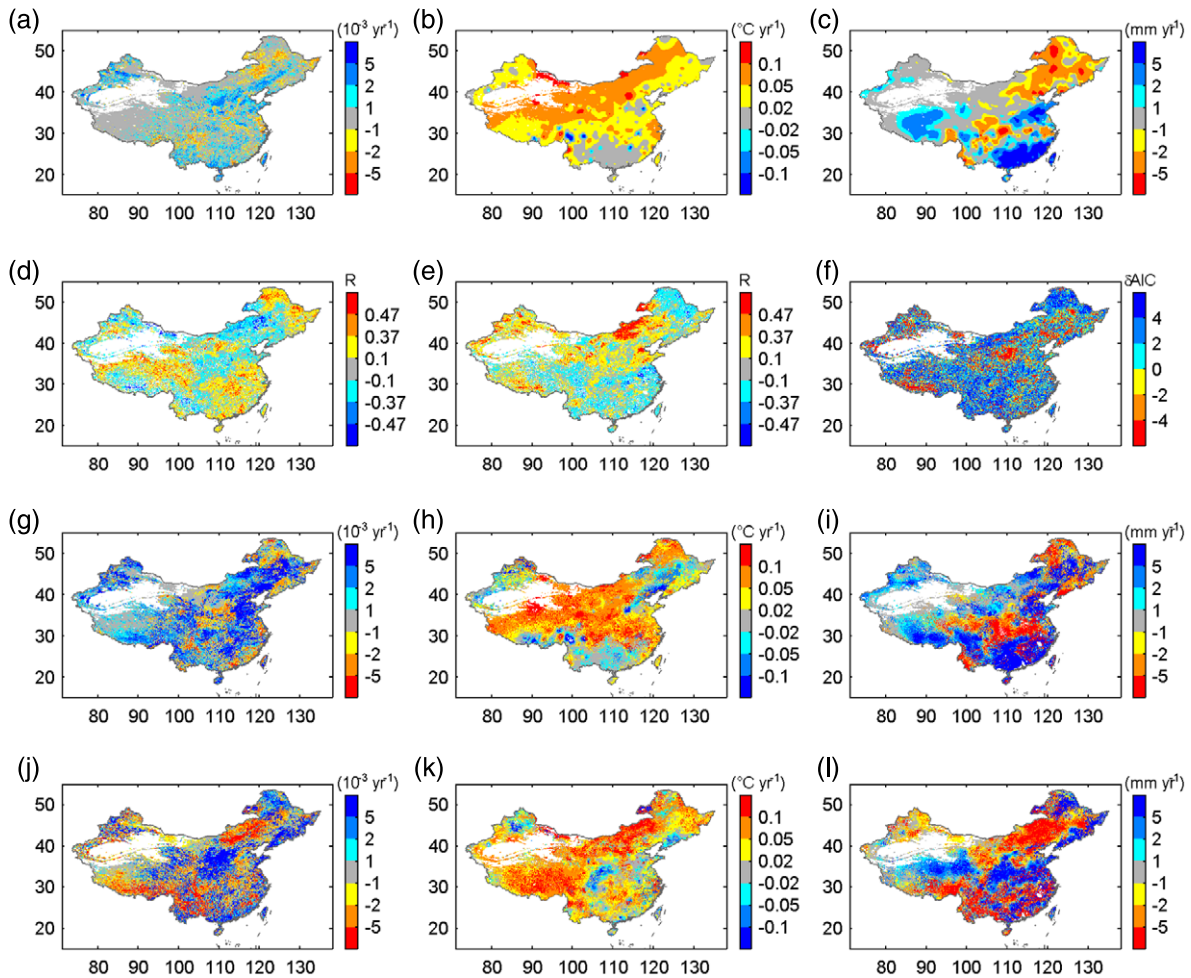


Figure 5. Spatial distribution of the results by the linear regression model and the piecewise regression model on June, July and August (JJA) NDVI and climate. Linear regression trends in JJA (a) NDVI, (b) temperature and (c) precipitation from 1982 to 2010. The correlation coefficients between JJA NDVI and (d) temperature and (e) precipitation. (f) Difference in AIC between piecewise regression and linear regression (ΔAIC). Trends in JJA NDVI (g) before and (j) after its TP. Trends in JJA temperature (h) before and (k) after the TP of the JJA NDVI trend. Trends in JJA precipitation (i) before and (l) after the TP of the JJA NDVI trend. $R = 0.37$ and $R = 0.47$ correspond statistically to 5% and 1% significance levels, respectively.

patterns as well. For example, in eastern Inner Mongolia, the decline of JJA NDVI (figure 5(j)) after the turning point is more remarkable than that of AM or SO NDVI, whereas in northeast China, the decrease in AM NDVI (figure 4(j)) after the turning point seems to be the most prominent. Overall, from 1982 to 2010, increasing seasonal NDVI was found in 69%, 57% and 68% of China’s land area for the AM, JJA and SO seasons, respectively (significant increase in 32%, 15% and 24% of the pixels, respectively), and the magnitude of the increased trend in the AM NDVI is larger than those of the JJA and SO NDVIs (figures 4(a), 5(a) and 6(a)).

This spatial variation in seasonal NDVI changes is closely linked with climate factors. The NDVI of AM is positively correlated with AM temperature in most of the study area (74% of the pixels), and significant positive correlation ($P < 0.05$) is observed in 28% of the pixels, mostly in central, east, north and northeast China as well as the Qinghai–Tibet Plateau (figure 4(d)). Spring warming could not only trigger an earlier onset of the growing season, but also stimulate photosynthetic rates, both of which enhance spring vegetation

activity (Tanja *et al* 2003, Richardson *et al* 2010). Thus, the increase in AM NDVI in central, east and south China of over 0.005 yr^{-1} can be partly explained by the significant increase in spring temperature ($>0.02 \text{ }^\circ\text{C yr}^{-1}$) in these regions where the precipitation is also plentiful (figures 4(a), (b) and (d)) (Piao *et al* 2010).

In contrast, without a concurrent increase in precipitation, warming in JJA may expedite evapotranspiration, increasing the JJA drought stress and thus inhibiting vegetation growth, especially in water-limited ecosystems (e.g. Angert *et al* 2005, Lotsch *et al* 2005, Bunn and Goetz 2006, Zhang *et al* 2008). Significantly positive correlations between NDVI and precipitation are found in more pixels for JJA (10%) than for AM (6%) and SO (3%). These pixels are mainly distributed in the arid and semi-arid regions of Inner Mongolia where JJA vegetation growth is primarily controlled by precipitation (figure 5(e)). In addition, the spatial patterns of trends in JJA NDVI match well with those in JJA precipitation both before and after the turning point of the JJA NDVI trend over these arid and semi-arid regions, especially in the east part of Inner

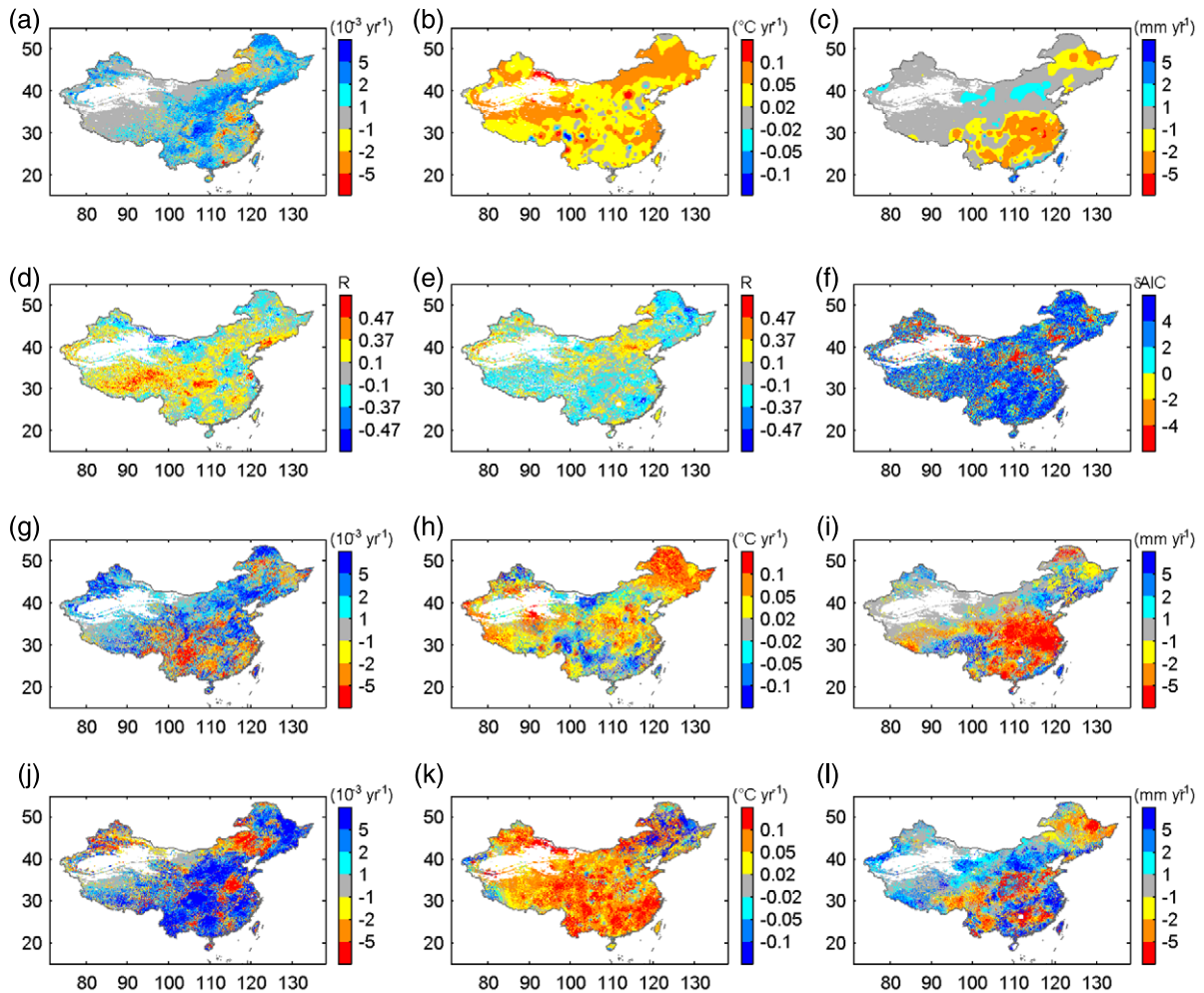


Figure 6. Spatial distribution of the results by the linear regression model and the piecewise regression model on September and October (SO) NDVI and climate. Linear regression trends in SO (a) NDVI, (b) temperature and (c) precipitation from 1982 to 2010. The correlation coefficients between SO NDVI and (d) temperature and (e) precipitation. (f) Difference in AIC between piecewise regression and linear regression (Δ AIC). Trends in SO NDVI (g) before and (j) after its TP. Trends in SO temperature (h) before and (k) after the TP of the SO NDVI trend. Trends in SO precipitation (i) before and (l) after the TP of the SO NDVI trend. $R = 0.37$ and $R = 0.47$ correspond statistically to 5% and 1% significance levels, respectively.

Mongolia (figures 5(g), (j), (i) and (l)), further confirming the critical role of precipitation in determining JJA vegetation activities in water-limited regions.

For the SO season, temperature significantly and positively correlated with SO NDVI in Qinghai–Tibet and central China (9% of our study area), while precipitation significantly and positively correlated with SO NDVI in northeast Inner Mongolia and north China (3% of our study area) (figures 6(d) and (e)). These climate driven patterns confirm that increased temperature in SO could enhance vegetation growth in cold regions and drought in arid and semi-arid regions could inhibit vegetation growth in SO (Piao *et al* 2006b, Suni *et al* 2003, Wan *et al* 2009).

3.3. Changes in NDVI over different ecosystems and their climate drivers

The changes in NDVI as a response to climate change are also different across different ecosystem types (figures 4–6). Table 2 shows the results of both linear and piecewise

regression on growing season NDVI for each ecosystem type. NDVI changes and their climate drivers share some similar patterns across most vegetation types to the general patterns described in the previous sections. We singled out those vegetation types showing different trends, while re-emphasizing the observed general pattern at the ecosystem level.

The growing season NDVI increased in all ecosystems except desert during 1982–2010. For the desert ecosystem, a significant turning point of the growing season NDVI is found in 1993 (table 2). Growing season NDVI significantly increased before 1993, but decreased after then (table 2). Growing season temperature significantly increased from 1982 to 2010 in all ecosystems except for desert, and NDVI in growing season is positively correlated with temperature in all ecosystems. In particular, this correlation is significant ($P < 0.05$) in EBF, ENF, DNF, shrubland, grassland, AMT and cropland ecosystems (table 2). In desert ecosystems, the reversal in growing season NDVI trend could

Table 2. Mean annual temperature (MAT, °C) and precipitation (MAP, mm), trends in growing season NDVI (0.01 yr^{-1}), temperature (Temp, °C yr^{-1}), and precipitation (Preci, mm yr^{-1}) during the whole period 1982–2010, turning point (TP) of growing season NDVI, difference in AIC between the piecewise regression model and the linear regression model (δAIC) for growing season NDVI, trends in NDVI (0.01 yr^{-1}), temperature (Temp, °C yr^{-1}), and precipitation (Preci, mm yr^{-1}) in the growing season before and after the TP of the growing season NDVI, and correlation coefficients between growing season NDVI and temperature (ENF) and precipitation (R_T) in evergreen broadleaf forests (EBF), deciduous broadleaf forests (DBF), broadleaf and needleleaf mixed forests (MF), evergreen needleleaf forests (ENF), deciduous needleleaf forests (DNF), shrubland, desert, grassland, alpine meadows and tundra (AMT) and cropland ecosystems over the period 1982 to 2010. * and ** stand for $P < 0.05$ and $P < 0.01$ (statistical significance of linear regression, piecewise regression or Pearson correlation), respectively.

Vegetation	MAT (°C)	MAP (mm)	Trend from 1982 to 2010						Trend before TP						Trend after TP						
			NDVI (10^{-2} yr^{-1})		Temp (°C yr^{-1})		Preci (mm yr^{-1})		δAIC	TP	NDVI (10^{-2} yr^{-1})		Temp (°C yr^{-1})		Preci (mm yr^{-1})		NDVI (10^{-2} yr^{-1})	Temp (°C yr^{-1})	Preci (mm yr^{-1})	R_T	R_P
			NDVI	Temp	NDVI	Temp	NDVI	Temp			Preci	Preci	NDVI	Temp	NDVI	Temp					
EBF	15.8	1259	0.09*	0.03**	0.8	2001	4.5	0.05	0.02	0.02	5.8*	0.22	0.08*	-15.1	0.32	-0.11					
DBF	6.2	621	0.07*	0.04**	-2.5*	2004	3.7	0.04	0.05**	-3.7*	0.25	0.02	0.7	0.28	-0.08						
MF	5.4	719	0.08*	0.04**	-2.2	1990	4.3	0.23	0.02	4.4	0.05	0.04*	-4.2	0.19	-0.12						
ENF	14.6	1163	0.12**	0.03**	0.7	2001	4.7	0.09	0.02	4.8*	0.21	0.09*	-14.8	0.49**	-0.10						
DNF	-1.5	474	0.11*	0.04**	-3.0*	1997	4.1	0.20*	0.05	-2.4	0.01	0.02	-3.3	0.42*	-0.35						
Shrubland	12.2	942	0.11**	0.03**	0.0	1988	4.7	0.22	0.01	-5.6	0.09*	0.04**	-0.7	0.50**	-0.05						
Desert	7.3	117	0.01	0.06**	0.4	1993**	-2.4	0.09**	0.00	1.1	-0.03	0.09**	-0.5	0.02	0.34						
Grassland	5.8	393	0.05**	0.05**	0.2	1988*	0.4	0.22*	0.04	-0.3	0.02	0.06**	-0.2	0.49**	0.51**						
AMT	3.3	385	0.04*	0.05**	0.2	1990*	-1.7	0.19**	0.04	2.2	0.00	0.06**	0.5	0.54**	0.09						
Cropland	12.4	826	0.12**	0.04**	-0.7	1988	1.6	0.40*	0.00	-7.4	0.07*	0.05**	-0.4	0.44*	0.02						

Table 3. Trends in seasonal NDVI (0.01 yr^{-1}), temperature (Temp, $^{\circ}\text{C yr}^{-1}$), and precipitation (Preci, mm yr^{-1}) during the whole period 1982–2010, turning point (TP) of seasonal NDVI, difference in AIC between the piecewise regression model and the linear regression model (δAIC) for seasonal NDVI, trends in seasonal NDVI (0.01 yr^{-1}), temperature (Temp, $^{\circ}\text{C yr}^{-1}$), and precipitation (Preci, mm yr^{-1}) before and after the TP of the seasonal NDVI, and correlation coefficients between seasonal NDVI and temperature (R_T) and precipitation (R_P) in the same season in evergreen broadleaf forests (EBF), deciduous broadleaf forests (DBF), broadleaf and needleleaf mixed forests (MF), evergreen needleleaf forests (ENF), deciduous needleleaf forests (DNF), shrubland, desert, grassland, alpine meadows and tundra (AMT) and cropland ecosystems over the period 1982–2010. * and ** stand for $P < 0.05$ and $P < 0.01$ (statistical significance of linear regression, piecewise regression or Pearson correlation), respectively.

Veg	Trend from 1982 to 2010				Trend before TP				Trend after TP				
	NDVI (10^{-2} yr^{-1})	T ($^{\circ}\text{C yr}^{-1}$)	P (mm yr^{-1})	TP	δAIC	NDVI (10^{-2} yr^{-1})	T ($^{\circ}\text{C yr}^{-1}$)	P (mm yr^{-1})	NDVI (10^{-2} yr^{-1})	T ($^{\circ}\text{C yr}^{-1}$)	P (mm yr^{-1})	R_T	R_P
April and May													
EBF	0.25**	0.03*	0.5	1994	4.7	0.13	0.03	-1.5	0.36*	0.03	0.3	0.42*	-0.27
DBF	0.12	0.03*	0.3	1998	2.0	0.27*	0.04	-0.5	-0.12	-0.02	0.1	0.71**	0.13
MF	-0.01	0.04	0.2	2002	2.9	0.13	0.07*	-0.7	-0.55	0.00	-1.0	0.73**	-0.37
ENF	0.28**	0.03**	0.3	1994	5.1	0.22	0.03	-1.3	0.31*	0.04	-0.3	0.48**	-0.29
DNF	0.14	0.03	0.1	1998	2.8	0.38	0.06	0.1	-0.20	0.01	-0.3	0.79**	-0.26
Shrub	0.24**	0.03**	0.3	1998	5.0	0.28**	0.04	-0.9	0.18	0.00	-2.3*	0.50**	-0.10
Desert	0.00	0.07**	0.1	1998*	-1.7	0.04*	0.06	-0.1	-0.07*	0.09	-0.5	0.03	0.18
Grassland	0.08**	0.05**	0.2	1998	3.8	0.11**	0.06*	-0.4	0.03	0.00	-0.5	0.65**	0.33
AMT	0.04*	0.05**	0.3**	1998**	-5.4	0.13**	0.07**	-0.2	-0.09*	0.03	0.1	0.64**	0.03
Cropland	0.20**	0.04*	0.2	1990	2.8	0.45*	-0.07	0.3	0.13*	0.08**	0.3	0.40*	0.26
June, July and August													
EBF	0.00	0.02**	1.5	1988	4.0	0.36	0.03	-5.2*	-0.05	0.03*	-0.1	0.03	-0.08
DBF	-0.02	0.04**	-1.7	2004*	-0.8	-0.08*	0.04*	2.5	0.37*	-0.08	4.4	0.06	0.13
MF	0.06	0.03*	-2.1	1988	2.2	0.41	0.01	2.2	0.00	0.02	-2.3	0.26	-0.14
ENF	0.03	0.02**	2.0	1988	3.0	0.31	0.06	-2.7	-0.01	0.03*	0.8	0.30	-0.03
DNF	0.01	0.04*	-2.7*	2004	3.2	-0.04	0.05*	-3.6*	0.36	-0.11	17.0	0.44*	-0.28
Shrub	0.03	0.03**	0.7	1988	1.8	0.31	0.05	-1.3	-0.01	0.03**	0.1	0.26	-0.07
Desert	0.01	0.06**	0.0	1988*	1.0	0.16*	0.06	1.7	-0.02	0.07**	-0.4	0.13	0.24
Grassland	0.02	0.05**	0.1	1988*	-0.6	0.30*	0.08	2.2	-0.02	0.05**	-0.4	0.18	0.52**
AMT	0.02	0.05**	0.1	1988*	0.6	0.29*	0.09	2.2	-0.02	0.05**	-0.1	0.43*	-0.06
Cropland	0.06	0.03*	0.2	1988**	-3.4	0.52**	0.05	-1.1	-0.01	0.03*	-0.3	0.19	0.17
September and October													
EBF	0.07	0.04**	-1.2*	2003	3.1	-0.03	0.03	-1.6	0.63	0.17	2.7	0.24	-0.09
DBF	0.15**	0.05**	-1.0**	2002	2.8	0.08	0.04	-1.3*	0.48*	0.10	-2.2	0.34	-0.48**
MF	0.21*	0.06**	-0.3	2003	1.1	0.07	0.06*	-0.2	0.94*	-0.02	-0.9	0.26	-0.24
ENF	0.09	0.04**	-1.5*	2001	3.2	-0.01	0.03	-1.8	0.40	0.15*	-4.5	0.27	-0.27
DNF	0.24**	0.04	-0.4	1997	4.8	0.32	0.06	-0.2	0.14	0.10	-0.9	-0.03	-0.39*
Shrub	0.10	0.04**	-0.9*	2001	3.5	0.03	0.03	-1.1	0.32	0.12	-2.2	0.27	-0.21
Desert	0.03*	0.05**	0.3*	1993	-5.4	0.12**	-0.02	-0.2	-0.02	0.09*	0.4	-0.14	0.27
Grassland	0.05*	0.05**	-0.2	1988	3.7	0.18	0.00	-1.3	0.03	0.05*	-0.1	0.36	-0.05
AMT	0.06**	0.05**	-0.2	1989	4.6	0.14	0.06	0.1	0.05	0.05**	-0.2	0.62**	0.08
Cropland	0.12**	0.04**	-1.0	2002	3.3	0.06	0.04	-1.9*	0.33	0.16*	-2.8	0.36	-0.29

be a result of simultaneously reversed precipitation change and continuously increased temperature (table 2), which is consistent with previous studies (Piao *et al* 2005, Zhang *et al* 2010, Jeong *et al* 2011, Piao *et al* 2011).

Table 3 summarizes the changes in seasonal NDVI and temperature and precipitation and the correlation coefficients between seasonal NDVI and temperature and precipitation in the concurrent seasons. For most vegetation types, both the AM and SO NDVIs significantly increased, while the JJA NDVI shows little trend from 1982 to 2010. This is in consistency with the findings at the national scale. For the JJA NDVI, significant trend change was found in DBF, desert, grassland, AMT and cropland ecosystems, but the piecewise regression model is only favored in cropland ecosystems ($\delta AIC = -3.4$).

The NDVI of AM is significantly correlated with the AM temperature in most ecosystems (table 3), suggesting that increase in AM temperature could enhance vegetation growth in AM for most vegetation types (e.g. (Piao *et al* 2006a, Richardson *et al* 2010)). The NDVI of JJA is mostly controlled by the JJA precipitation for most vegetation types. The reversed JJA NDVI trend for desert, grassland, AMT and cropland ecosystems (table 3) could be due to drought stress resulting from decreased precipitation but increased temperature after the turning point. The critical control by precipitation for the JJA NDVI is particularly obvious in grassland ecosystems ($R = 0.52$, $P = 0.004$), which is consistent with the observation in Eurasia that decrease in JJA precipitation along with increase in JJA temperature after the 1990s inhibited the vegetation growth in arid and semi-arid regions (Park and Sohn 2010, Piao *et al* 2011). A warming experiment in the semi-arid grassland ecosystem in Inner Mongolia suggested that daytime warming could inhibit vegetation growth because of the warming induced drought stress (Wan *et al* 2009). The NDVI of SO is positively but marginally correlated with the SO temperature in most ecosystems except for DNF and desert ecosystems, suggesting that increase in SO temperature could enhance vegetation growth owing to the prolonged growing season (Churkina *et al* 2005, Piao *et al* 2006a).

4. Conclusions and future directions

In this study, by using both linear and piecewise regression models, we show that the growing season NDVI increased in central and southern China from 1982 to 2010, while in northern China (i.e. Inner Mongolia, northwest and northeast China) a significant change in growing season NDVI trend occurred in the 1990s and early 2000s. The increase in growing season NDVI before the 1990s may result from the warming trend and more precipitation during the period from 1982 to the mid 1990s, which enhanced vegetation growth (Piao *et al* 2003, 2011), while the decrease in the growing season NDVI after the 1990s or early 2000s, especially over the arid and semi-arid regions in northern China, can be attributed to drought stress strengthened by warming and less precipitation (Angert *et al* 2005, Lotsch *et al* 2005, Park and Sohn 2010).

China is projected to experience an increase in temperature of 1–5 °C and an accompanying increase in summer precipitation of $7 \pm 7\%$ over the next century (Piao *et al* 2010). An understanding of the vegetation response to the projected future climate change provides a vital scientific base for China's environmental and climate change policies. Our study suggests that the enhanced vegetation growth in the 1980s and 1990s may not persist, especially in the arid and semi-arid ecosystems, owing to drought stress, which could reduce the carbon uptake by vegetation (Angert *et al* 2005, Zhao and Running 2010). However, the responses of vegetation growth to climate changes are nonlinear and also involve complicated interactions among different climate factors (Zhang *et al* 2010, Piao *et al* 2011). Long-term *in situ* and satellite observations of vegetation growth and climate change as well as ecosystem modeling studies are urgently needed. Furthermore, apart from climate change, recovery from disturbance, land use/cover change, rising CO₂ concentration and nitrogen deposition also contribute to changes in vegetation growth (Piao *et al* 2009, Tian *et al* 2011, Beck and Goetz 2011). It is nearly impossible to predict the future vegetation growth and carbon sinks without a mechanistic terrestrial ecosystem processes model integrating all the main factors such as climate change, rising CO₂ concentration, nitrogen deposition, ozone pollution and aerosols.

Acknowledgments

This study was supported by the National Natural Science Foundation of China (grants 41125004 and 30970511), Foundation for Sino–EU research cooperation of the Ministry of Science and Technology of China (1003), CARBONES EU FP7 foundation (242316), Foundation for the Author of National Excellent Doctoral Dissertation of PR China (FANEDD-200737) and National Basic Research Program of China (Grant No. 2010CB950601).

References

- Angert A, Biraud S, Bonfils C, Henning C C, Buermann W, Pinzon J, Tucker C J and Fung I 2005 Drier summers cancel out the CO₂ uptake enhancement induced by warmer springs *Proc. Natl Acad. Sci. USA* **102** 10823–7
- Beck H E, McVicar T R, van Dijk A I J M, Schellekens J, de Jeu R A M and Bruijnzeel L A 2011 Global evaluation of four AVHRR–NDVI data sets: intercomparison and assessment against Landsat imagery *Remote Sens. Environ.* **115** 2547–63
- Beck P S A and Goetz S J 2011 Satellite observations of high northern latitude vegetation productivity changes between 1982 and 2008: ecological variability and regional differences *Environ. Res. Lett.* **6** 045501
- Bunn A G and Goetz S J 2006 Trends in satellite-observed circumpolar photosynthetic activity from 1982 to 2003: the influence of seasonality, cover type, and vegetation density *Earth Interact.* **10** 1–20
- Burnham K P and Anderson D R 2002 *Model Selection and Multimodel Inference: A Practical Information-Theoretic Approach* (Berlin: Springer)
- Churkina G, Schimel D, Braswell B H and Xiao X 2005 Spatial analysis of growing season length control over net ecosystem exchange *Glob. Change Biol.* **11** 1777–87

- Ding Y H, Ren G Y, Zhao Z C, Xu Y, Luo Y, Li Q P and Zhang J 2007 Detection, causes and projection of climate change over China: an overview of recent progress *Adv. Atmos. Sci.* **24** 954–71
- Editorial Board of Vegetation Map of China, Chinese Academy of Sciences 2001 *Vegetation Atlas of China* (Beijing: Science Press)
- Goetz S J, Bunn A G, Fiske G J and Houghton R A 2005 Satellite-observed photosynthetic trends across boreal North America associated with climate and fire disturbance *Proc. Natl Acad. Sci. USA* **102** 13521–5
- Hansen J, Ruedy R, Sato M and Lo K 2010 Global surface temperature change *Rev. Geophys.* **48** RG4004
- Holben B N 1986 Characteristics of maximum-value composite images from temporal AVHRR Data *Int. J. Remote Sens.* **7** 1417–34
- Jeong S J, Ho C H, Brown M E, Kug J S and Piao S L 2011 Browning in desert boundaries in Asia in recent decades *J. Geophys. Res.—Atmos.* **116** D02103
- Lin D, Xia J and Wan S 2010 Climate warming and biomass accumulation of terrestrial plants: a meta-analysis *New Phytol.* **188** 187–98
- Lotsch A, Friedl M A, Anderson B T and Tucker C J 2005 Response of terrestrial ecosystems to recent northern hemispheric drought *Geophys. Res. Lett.* **32** L06705
- McMahon S M, Parker G G and Miller D R 2010 Evidence for a recent increase in forest growth *Proc. Natl Acad. Sci. USA* **107** 3611–5
- Myneni R B, Keeling C D, Tucker C J, Asrar G and Nemani R R 1997 Increased plant growth in the northern high latitudes from 1981 to 1991 *Nature* **386** 698–702
- Niu S, Luo Y, Fei S, Montagnani L, Bohrer G, Janssens I A, Gielen B, Rambal S, Moors E and Matteucci G 2011 Seasonal hysteresis of net ecosystem exchange in response to temperature change: patterns and causes *Glob. Change Biol.* **17** 3102–14
- Pan Y et al 2011 A large and persistent carbon sink in the world's forests *Science* **333** 988–93
- Park H S and Sohn B J 2010 Recent trends in changes of vegetation over East Asia coupled with temperature and rainfall variations *J. Geophys. Res.—Atmos.* **115** D14101
- Piao S L, Ciais P, Friedlingstein P, de Noblet-Ducoudre N, Cadule P, Viovy N and Wang T 2009 Spatiotemporal patterns of terrestrial carbon cycle during the 20th century *Glob. Biogeochem. Cycle* **23** GB4026
- Piao S L, Fang J Y, Liu H Y and Zhu B 2005 NDVI-indicated decline in desertification in China in the past two decades *Geophys. Res. Lett.* **32** L06402
- Piao S L, Fang J Y, Zhou L M, Ciais P and Zhu B 2006a Variations in satellite-derived phenology in China's temperate vegetation *Glob. Change Biol.* **12** 672–85
- Piao S L, Fang J Y, Zhou L M, Guo Q H, Henderson M, Ji W, Li Y and Tao S 2003 Interannual variations of monthly seasonal normalized difference vegetation index (NDVI) in China from 1982 to 1999 *J. Geophys. Res.—Atmos.* **108** 4401–13
- Piao S L, Mohammad A, Fang J Y, Cai Q and Feng J M 2006b NDVI-based increase in growth of temperate grasslands and its responses to climate changes in China *Glob. Environ. Change—Hum. Policy Dimens.* **16** 340–8
- Piao S L, Wang X H, Ciais P, Zhu B, Wang T and Liu J 2011 Changes in satellite-derived vegetation growth trend in temperate boreal Eurasia from 1982 to 2006 *Glob. Change Biol.* **17** 3228–39
- Piao S L et al 2010 The impacts of climate change on water resources and agriculture in China *Nature* **467** 43–51
- Richardson A D et al 2010 Influence of spring and autumn phenological transitions on forest ecosystem productivity *Phil. Trans. R. Soc. B* **365** 3227–46
- Slayback D A, Pinzon J E, Los S O and Tucker C J 2003 Northern hemisphere photosynthetic trends 1982–99 *Glob. Change Biol.* **9** 1–15
- Suni T, Berninger F, Markkanen T, Keronen P, Rannik U and Vesala T 2003 Interannual variability and timing of growing-season CO₂ exchange in a boreal forest *J. Geophys. Res.—Atmos.* **108** 4265
- Tanja S et al 2003 Air temperature triggers the recovery of evergreen boreal forest photosynthesis in spring *Glob. Change Biol.* **9** 1410–26
- Tian H et al 2011 China's terrestrial carbon balance: contributions from multiple global change factors *Glob. Biogeochem. Cycles* **25** GB1007
- Toms J D and Lesperance M L 2003 Piecewise regression: a tool for identifying ecological thresholds *Ecology* **84** 2034–41
- Tucker C J, Pinzon J E, Brown M E, Slayback D A, Pak E W, Mahoney R, Vermote E F and El Saleous N 2005 An extended AVHRR 8-km NDVI dataset compatible with MODIS and SPOT vegetation NDVI data *Int. J. Remote Sens.* **26** 4485–98
- Wan S, Xia J, Liu W and Niu S 2009 Photosynthetic overcompensation under nocturnal warming enhances grassland carbon sequestration *Ecology* **90** 2700–10
- Wang X H, Piao S L, Ciais P, Li J S, Friedlingstein P, Koven C and Chen A P 2011 Spring temperature change its implication in the change of vegetation growth in North America from 1982 to 2006 *Proc. Natl Acad. Sci. USA* **108** 1240–5
- Zhang K, Kimball J S, Hogg E H, Zhao M S, Oechel W C, Cassano J J and Running S W 2008 Satellite-based model detection of recent climate-driven changes in northern high-latitude vegetation productivity *J. Geophys. Res.—Biogeosci.* **113** G03033
- Zhang X Y, Goldberg M, Tarpley D, Friedl M A, Morisette J, Kogan F and Yu Y Y 2010 Drought-induced vegetation stress in southwestern North America *Environ. Res. Lett.* **5** 024008
- Zhao M S and Running S W 2010 Drought induced reduction in global terrestrial net primary production from 2000 through 2009 *Science* **329** 940–3
- Zhou L, Kaufmann R K, Tian Y, Myneni R B and Tucker C J 2003 Relation between interannual variations in satellite measures of northern forest greenness climate between 1982 and 1999 *J. Geophys. Res.—Atmos.* **108** 4004–20
- Zhou L M, Tucker C J, Kaufmann R K, Slayback D, Shabanov N V and Myneni R B 2001 Variations in northern vegetation activity inferred from satellite data of vegetation index during 1981 to 1999 *J. Geophys. Res.—Atmos.* **106** 20069–83